ACS Photonics

pubs.acs.org/journal/apchd5

Article

# Resonant Light Trapping via Lattice-Induced Multipole Coupling in Symmetrical Metasurfaces

Alexei V. Prokhorov, Pavel D. Terekhov, Mikhail Yu. Gubin, Alexander V. Shesterikov, Xingjie Ni, Vladimir R. Tuz, and Andrey B. Evlyukhin*

Cite This: https://doi.org/10.1021/acsphotonics.2c01066

Read Online

ACCESS | Metrics & More | Article Recommendations | Supporting Information

**ABSTRACT:** We demonstrate a general multipole mechanism of the resonant mode trapping effect in metasurfaces composed of $MoS_2$ disk-shaped nanoresonators. The implementation of this mechanism does not require any special irradiation conditions for the incident light or geometrical distortion of the symmetry of the metasurface translation unit cell. It is established that the effect arises due to the periodic-lattice-induced coupling between the electric dipole and electric octupole modes existing in the nanoresonators. We show that, under these conditions, the resonant quasi-trapped octupole mode and the suppression of the electric dipole response can be self-consistently realized under the action of normally incident plane waves. This, in turn, leads to the appearance of a narrow-band-induced transparency of the metasurface supplemented by the strong electromagnetic energy storage in the nanoresonators. Due to its general nature, the presented mechanism can be implemented in various dielectric and semiconductor metasurfaces, whose meta-atoms support resonant excitation conditions for different-order multipole moments with the same inverse symmetry property.

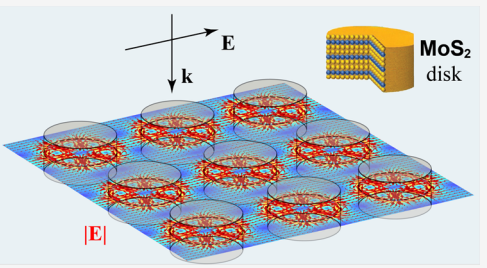


**KEYWORDS:** *Mie resonances, metasurfaces, nanoparticles, multipoles, trapped modes*



## INTRODUCTION

Modern technologies of light control are one of the key drivers in the fields of energy harvesting, microelectronics, and microbiology. Advanced photonic technologies rely on increasing the integration level of individual photonic elements up to the level suitable for creating "smart" materials (metamaterials), where functions of storing, processing, and routing the electromagnetic energy flow are encapsulated inside a single device.[1−6] The "meta-atoms" of such metamaterials are optimized for solving specific tasks. Thus, the use of metallic and dielectric nanoparticles supporting localized plasmon[7,8] and Mie resonances[9−12] provides direct possibilities for the amplitude-phase manipulation of light propagation at various spatial scales.

In particular, due to electromagnetic interactions between meta-atoms arranged in periodic lattices, metamaterials with a thickness of one layer of nanoparticles, called metasurfaces, can support narrow-band collective resonances associated with the excitation of quasi-trapped modes,[13−15] which, in turn, are a practical realization of bound states in the continuum (BICs).[16,17] Such states are applicable for solving various problems including the high-harmonics generation,[18−20] nonlinear optical operations,[21,22] and light trapping and mode selection[23] in two-dimensional laser systems[24−27] with a decreased lasing threshold.[28,29]

True BICs with infinite quality factors are related to eigenstates whose fields are perfectly localized inside an optical system without any radiation into free space. In the concept of metasurfaces, they are purely real eigenstates existing in idealized lossless infinitely expanded structures whose translation unit cells possess a specific spatial symmetry. To excite the corresponding eigenstate by the field of the incident radiation, a specific perturbation should be introduced into the unit cells, which breaks their symmetry transforming the eigenstate conditions from BIC to quasi-BIC. This transformation manifests itself in the metasurface spectra as a resonance with a quality factor depending on the degree of the introduced asymmetry.[30−35] The use of specific irradiation conditions (structured light, near-field sources, etc.) is another possible way to realize quasi-BIC excitation in metasurfaces.[29,36] Nevertheless, for both these cases, the implementation of the high-quality factor resonances requires special tuning or modification of the properties of the overall optical system.

In this paper, we propose an efficient strategy for the excitation of high-quality factor quasi-trapped mode resonances without the need for introducing perturbations into unit cells of the metasurface or specific irradiation conditions

Received: July 9, 2022

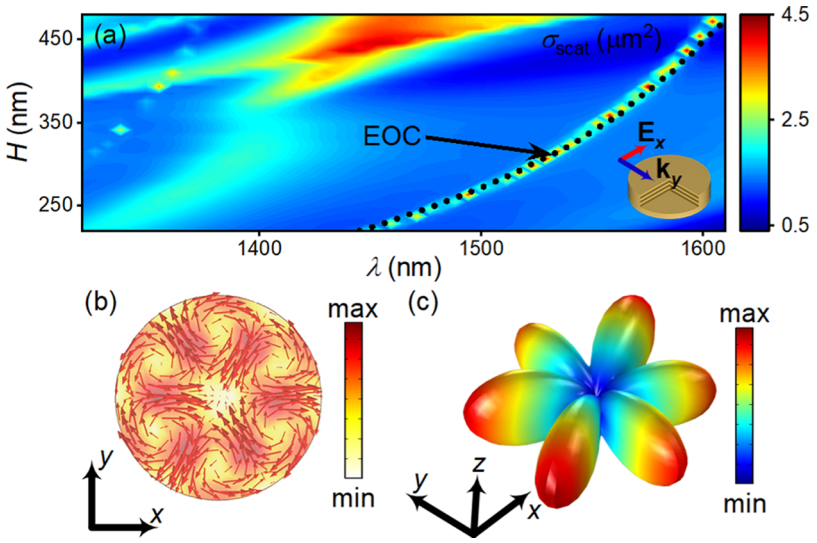


**Figure 1.** (a) $\lambda-H$ map of the scattering cross sections calculated for single $MoS_2$ disks with the fixed radius $R_d$ = 418 nm. The disks are irradiated from the side by plane waves with electric polarization directed parallel to the disk bases. Here, $H$ is the disk height and $\lambda$ is the incident wavelength. The dotted black curve corresponds to the $\lambda-H$ dependence of the octupole eigenstate. (b) The distribution of electric energy flows and (c) radiation pattern related to the octupole eigenstate of a disk with $H$ = 418 nm at the wavelength $\lambda_{oct}$ = 1587 nm.

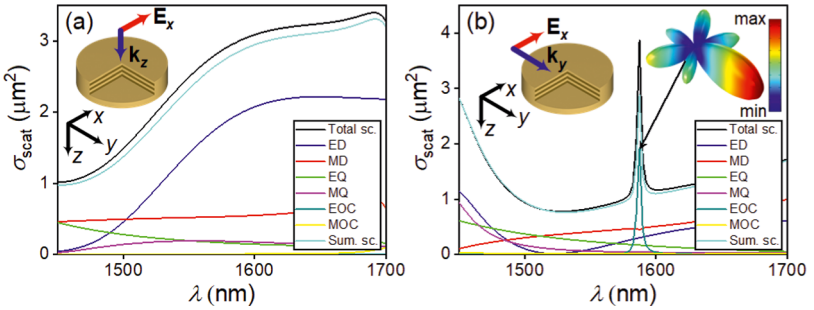


**Figure 2.** Scattering cross section for the $MoS_2$ disk (a) normally ($k_z$) and (b) laterally ($k_y$) irradiated by the $x$-polarized ($E_x$) wave. "Total sc." and "Sum sc." correspond to the scattering cross section calculated by direct numerical simulation and by the summation of multipole moment contributions, respectively: electric (ED) and magnetic (MD) dipoles, electric (EQ) and magnetic (MQ) quadrupoles, and electric (EOC) and magnetic (MOC) octupoles. The insets indicate the irradiation conditions. The inset in panel (b) presents the far-field scattering pattern at the EOC resonance.

for the incident light. This strategy is based on the periodic-lattice-induced energy coupling in the metasurface implemented between the nanoparticle's multipole moments with the same inverse symmetry.[37] The feature of the system under consideration is associated with the self-consistent realization of the induced transparency effect and the trapped mode regime resulting in the electromagnetic energy storage inside the metasurface. We discuss in detail how the trapped mode can be reached via the coupling between the electric dipole and electric octupole moments in the example of the metasurface composed of disk-shaped nanoparticles. It is shown that the protection of such a state from decay is associated with the coupling-induced suppression of the electric dipole moments under conditions of the resonant enhancement of the octupole moments.

## OCTUPOLE RESONANCE IN AN ISOLATED DISK

We start with the study of the optical properties of a single nanoparticle (disk) behaving as a meta-atom of our metasurface. For definiteness, but without the loss of generality, we further assume that the disk is made of a bulk $MoS_2$ material. In the $MoS_2$ material, the layers are disposed parallel to the disk bases, and its permittivity is known from experimental data (see ref 38 and Figure S1). Our choice of this material is due to the fact that $MoS_2$ has a relatively high value of permittivity and low material losses in the selected operating wavelength range (the generality of our consideration is also confirmed by our calculations for Si disks; see Figures S2 and S3). For all our subsequent numerical simulations, we use the COMSOL Multiphysics electromagnetic solver.

To find a corresponding mode, we consider the scattering spectra of the $x$-polarized wave incident laterally on the disk (see the inset in Figure 1a). In our calculations, we fix the disk's radius $R_d$ and vary the disk's height $H$ versus the wavelength $\lambda$ of the incident radiation. The resulting $\lambda-H$ map of the scattering cross section $\sigma_{scat}$ presented in Figure 1a demonstrates a narrow resonant feature existing within the third telecommunication window. The eigenwave analysis proves that this resonance is associated with the excitation of the electric octupole eigenstate of a cylindrical resonator ($TE_{31\delta}$ mode). It follows from the facts that (i) the spectral positions of this eigenstate for the disks with different heights (presented by black dots in Figure 1a) correspond exactly with the resonant curve of $\sigma_{scat}$ and (ii) the multipole expansion of


https://doi.org/10.1021/acsphotonics.2c01066
ACS Photonics XXXX, XXX, XXX−XXX

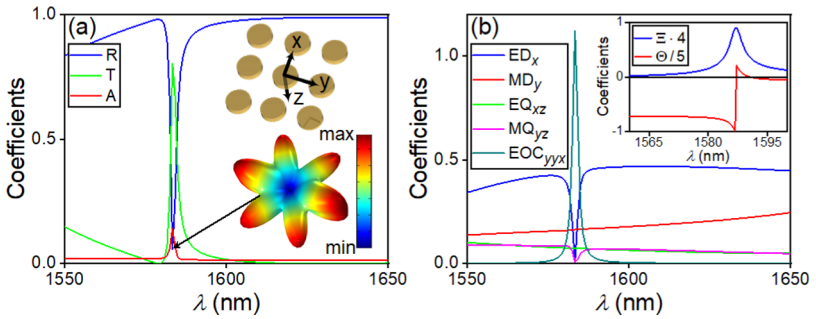


**Figure 3.** (a) Reflection ($R$), transmission ($T$), and absorption ($A$) coefficients for the metasurface with period $P$ = 1121 nm composed of $MoS_2$ disks with parameters as in Figure 2 and irradiated by the wave with $E_x$ and $k_z$. (b) Spectra of the absolute values of the multipole contributions in the reflection coefficient given by eq 1, as well as the value $EOC_{yyx}$ corresponding to the EOC moment of the disks in the metasurface. The insets: (a) a fragment of the infinite metasurface with the Cartesian coordinate system; the radiation pattern from a unit cell at the resonant wavelength $\lambda_R$; and (b) spectra of coefficients Ξ and Θ calculated by eq 8a.

the eigenstate contains the electric octupole (EOC) moment as the main multipole contribution. Moreover, the electric field distribution (Figure 1b) plotted for a particular disk height ($H$ = 418 nm) and the radiation pattern (Figure 1c) calculated for this eigenstate explicitly correspond to the behavior of the EOC moment. The multipole analysis of the scattering cross sections also confirms that the narrow maxima in Figure 1a correspond to the resonant excitation of the electric octupole moment of the disk (the main equations of the multipole analysis can be found in the Supporting Information).

In the following consideration, we focus our attention on the $MoS_2$ disk with geometric sizes of $R_d = H$ = 418 nm. Such a single disk, placed in air ($\varepsilon_d$ = 1) and normally irradiated by the $x$-polarized wave, has a smooth dependence of scattering cross section without singularities in the wavelength range of 1480−1700 nm (see Figure 2a). Whereas under the lateral irradiation, the narrow-band feature appears at the resonant wavelength $\lambda_{oct}$ = 1587 nm, which corresponds to the resonant excitation of the disk octupole moment (see the multipole contributions into the total scattering cross section in Figure 2b). In this case, the radiation pattern demonstrates the propagation of scattered waves only in the $xy$-plane (see the inset in Figure 2b). The electric dipole contribution to the scattering cross sections does not have any narrow spectral feature for the normal and lateral irradiation conditions.

Note that the incident electric field for both irradiation conditions has the same polarization; however, the octupole resonance is excited only in the lateral geometry. This feature can be explained by means of multipole analysis of the disk eigenstates and the incident wave. Indeed, the excitation of the octupole resonance corresponds to the excitation of the disk octupole eigenstate, the multipole composition of which is basically presented by the electric octupole term (see Figure 1b,c). The resonant coupling between the external wave and octupole eigenstate may occur only if the multipole expansion of the external wave contains the corresponding octupole term. The multipole expansion of the $x$-polarized plane wave has the corresponding octupole term only for the lateral geometry (see Figure S4), so it is the case when octupole resonance is excited in the disk.

## OCTUPOLE MODE TRAPPING IN A METASURFACE

Let us combine the considered disks into a subdiffractive infinite metasurface with a period $P_{oct}$ = 1121 nm, which we have chosen after some optimization procedure with respect to the quality factor of the resonant features of the reflection spectra. The Cartesian coordinate system is chosen so that the metasurface is located in the $xy$-plane, with the origin coinciding with the center of one of the disks. The reflection, transmission, and absorption spectra of the metasurface normally (along the $z$-axis) irradiated by the $E_x$-polarized plane wave are presented in Figure 3a. We observe a narrow dip almost approaching zero in the reflection spectrum at the wavelength $\lambda_R$ = 1588 nm with a simultaneous increase of the absorption. The radiation pattern of each disk in the metasurface for this wavelength has a bright octupole character (see the inset in Figure 3a) and corresponds to the energy propagation only along the metasurface plane. Figure 3b shows the relative contributions of all nonzero components of electric $ED_x = |Kp_x|^2$ and magnetic $MD_y = |Km_y/\upsilon_d|^2$ dipole moments $p_x$ and $m_y$, electric $EQ_{xz} = |KQ_{xz}ik_d/6|^2$ and magnetic $MQ_{yz} = |KM_{yz}ik_d/(2\upsilon_d)|^2$ quadrupole moments $Q_{xz}$ and $M_{yz}$ to the total light reflection coefficient $R$ of the metasurface. In our case, this coefficient, accounting for the main multipole moments providing the reflection, is determined by the $\upsilon$expression[39]

$$R \simeq \left| K\left(p_x - \frac{m_y}{\upsilon_d} + \frac{ik_d}{6}Q_{xz} - \frac{ik_d}{2\upsilon_d}M_{yz}\right)\right|^2 \quad (1)$$

where $K = ik_d/(E_x^0 2S_L\varepsilon_0\varepsilon_d)$, $S_L = P^2$ is the area of a lattice unit cell, $k_d = k_0\sqrt{\varepsilon_d}$ and $\upsilon_d = 1/\sqrt{\varepsilon_0\mu_0\varepsilon_d}$ are the wave number and speed of light in the surrounding medium with permittivity $\varepsilon_d$, respectively, $k_0$ is the wave number in the vacuum, $E_x^0$ is the electric field of the incident wave in the metasurface plane, $\varepsilon_0$ is the vacuum permittivity, and $\mu_0$ is the vacuum permeability.

It is revealed that the dip in the reflection spectrum in Figure 3a is associated with the complete suppression of the main component of the electric dipole moment $p_x$ of each disk at the wavelength $\lambda_R$. For comparison, Figure 3b shows the value $EOC_{yyx} = |KO_{yyx}k_d^2/6|^2$ corresponding to the resonant component $O_{yyx}$ of the EOC moment, which does not give any contribution to the reflection coefficient and corresponds to the excitation of octupole eigenstates in each disk (see Figure 1). Further, we will show that the suppression of the dipole component $p_x$ at the wavelength $\lambda_R$ and the corresponding reflection suppression is a result of dipole−octupole coupling in the metasurface array.

In fact, the octupole mode is not directly excited in the single disk under frontal incidence conditions. Therefore, we should conclude that excitation becomes possible in the metasurface due to the electromagnetic interaction (coupling) between all its disks forming the array (see Figure S5 and the


https://doi.org/10.1021/acsphotonics.2c01066
ACS Photonics XXXX, XXX, XXX−XXX

corresponding analysis of the coupling effect in the finite size array in the Supporting Information). We suppose that due to the interparticle interaction, the high-quality factor resonant octupole mode of every disk of the array interacts with the broad electric dipole mode of other disks. Due to this interaction, there is an energy flow between the dipole mode, excited by external waves in the metasurface's disks, and their octupole mode. Therefore, the dipole mode serves as a channel for energy transfer from external waves to the octupole mode. From the numerical simulations, we see that the resonant excitation of the octupole mode leads to a significant decrease of the disks' electric dipole moment, indicating that the dipole mode ceases to be excited. In this condition, the energy stored in the octupole mode is distributed in the metasurface plane. Such a process could be imagined as light trapping in the octupole disk mode.

Note that the resonant suppression of the electric dipole moments of all disks in the array cannot be related to the excitation of their anapole states.[40] From the single-particle response presented in Figure 2, it is clear that the total ED contribution does not have a local minimum at the point of EOC resonance and monotonically increases with wavelength for frontal and lateral irradiation conditions. It means that (i) the single-particle ED polarizability $\hat{\alpha}_p$ is not equal to zero at the EOC resonance in the array, and the anapole state of single particles does not have a relation to the ED suppression in the array, and (ii) the ED suppression is a result of the multipole coupling in the array.

Theoretically, the light trapping effect in the disk octupole mode can be clarified in the framework of the lattice dipole−quadrupole−octupole coupling model. In this model, each dipole (high-order multipole) moment of each disk in the array is determined by the corresponding single-particle polarizability tensor and the local electric or magnetic fields (the field derivatives) acting on this disk and determined by a superposition of the external wave fields and the fields radiated by multipoles of other disks. In this approach, for example, the coupling between an electric dipole and other multipoles means that the electric fields of the multipoles make a nonzero contribution to the local electric field at the localization point of the electric dipole and can affect its magnitude and direction. Note that in periodic arrays of particles (metasurfaces), only odd multipoles can make such a nonzero contribution to local electric fields since they radiate waves in the forward and backward directions with the same phase. Mathematically, similar to the approach recently discussed,[37] equations for the electric dipole $\mathbf{p}$ and electric octupole $\hat{O}$ moments of each disk in an infinite 2D periodic array normally irradiated by a linearly polarized plane wave with the electric field amplitude $\mathbf{E}^0$ can be written as

$$\mathbf{p} = \hat{\alpha}_p \mathbf{E}^0 + \hat{\alpha}_p \left( \sum_{l\neq 0}^{\infty} \hat{G}_l \right) \mathbf{p} + \hat{\alpha}_p \left( \sum_{l\neq 0}^{\infty} \hat{H}_l \right) \hat{M} + \hat{\alpha}_p \left( \sum_{l\neq 0}^{\infty} \hat{P}_l \right) \hat{O} \tag{2}$$

$$\hat{O} = \hat{\alpha}_O \left( \sum_{l\neq 0}^{\infty} \hat{D}_l \right) \mathbf{p} + \hat{\alpha}_O \left( \sum_{l\neq 0}^{\infty} \hat{L}_l \right) \hat{M} + \hat{\alpha}_O \left( \sum_{l\neq 0}^{\infty} \hat{F}_l \right) \hat{O} \tag{3}$$

where $\hat{\alpha}_p$ and $\hat{\alpha}_O$ are the electric dipole and octupole polarizability tensors of the single disk, respectively, $\hat{M}$ is the disk's MQ moment; the values in parentheses present the tensors of the lattice ED, MQ-ED, EOC-ED, ED-EOC, MQ-EOC, and EOC sums, respectively, $l$ is the number of the disk in the metasurface; the sums do not include the disk located at the origin of the Cartesian coordinate system (see the inset in Figure 3a). Equations 2 and 3 take into account the facts that (i) the multipole moments of all disks in the metasurface are the same under the chosen irradiation conditions and (ii) the multipole coupling in the periodic arrays can exist only between the multipole of the same parity under inversion (in our case, between the odd multipole moments: $\mathbf{p}$, $\hat{M}$, and $\hat{O}$). Since the contribution of the MQ moment to the reflection and transmission coefficients is nonresonant and weak (Figure 3), we do not explicitly consider the equation for $\hat{M}$. Note that eq 3 includes only the coupling terms since the octupole resonant mode cannot be excited directly by the normally incident plane wave.

From Figure 3b, one can conclude that $\mathbf{p} \to 0$ and $\hat{M} \to 0$ at the $\lambda_R$ = 1588 nm of the EOC resonance. Therefore, the system of eqs 2 and 3 at the $\lambda_R$ is written as

$$\hat{\alpha}_p \mathbf{E}^0 = -\hat{\alpha}_p \left( \sum_{l\neq 0}^{\infty} \hat{P}_l \right) \hat{O} \tag{4}$$

$$\hat{O} = \hat{\alpha}_O \left( \sum_{l\neq 0}^{\infty} \hat{F}_l \right) \hat{O} \tag{5}$$

where the first and second equations are the mode trapping condition and the equation of the octupole trapped mode, respectively. Physically, this means that the summed electric field at the coordinate system origin, created by resonant electric octupole moments of all disks except the disk located at the origin, excites in this disk an electric dipole moment equal in magnitude and opposite in phase to the dipole moment excited by the external wave (eq 4). This leads to the suppression of the total electric dipole moment of the disk located at the origin of the coordinate system. Since, due to translation symmetry (periodicity), all disks in the metasurface are under equivalent irradiation conditions, the suppression of the dipole moment applies to all disks. This, in turn, leads to the suppression of the reflection from the metasurface and the appearance of induced transparency under the EOC resonance ($\lambda_R$ = 1588 nm in Figure 3). Since the excited EOC moments do not radiate electromagnetic waves beyond the metasurface, the energy corresponding to them is stored in the metasurface plane and the octupole mode trapping effect (eq 5) is realized. It is seen from eq 4 that the condition for realization of the trapping effect is destroyed if the external (incident) field disappears. Indeed, if the external field is switched off ($\mathbf{E}^0 = 0$), then the system with eqs 4 and 5 can be satisfied only at $\hat{O} = 0$. We emphasize that the nontrivial solution of eq 5 cannot be an eigenstate of the metasurface since, owing to the dipole−octupole coupling always existing in the metasurface, the multipole decomposition of the corresponding eigenmode must also include the dipole terms. Thus, the nontrivial solution of eq 5 can be considered as a quasi-trapped mode being a result of an amplitude-phase self-consistent response of the metasurface to the external light wave.

As follows from the numerical simulations of the metasurface optical response, the traceless tensor $\hat{O}$ of EOC moment is represented by only two components $O_{yyx}$ and $O_{xxx}$, which are related by the equality $O_{yyx} = -O_{xxx}$. Therefore, in the approximation of the only far-field coupling, eq 4 can be estimated as (see the Supporting Information)


https://doi.org/10.1021/acsphotonics.2c01066
ACS Photonics XXXX, XXX, XXX−XXX

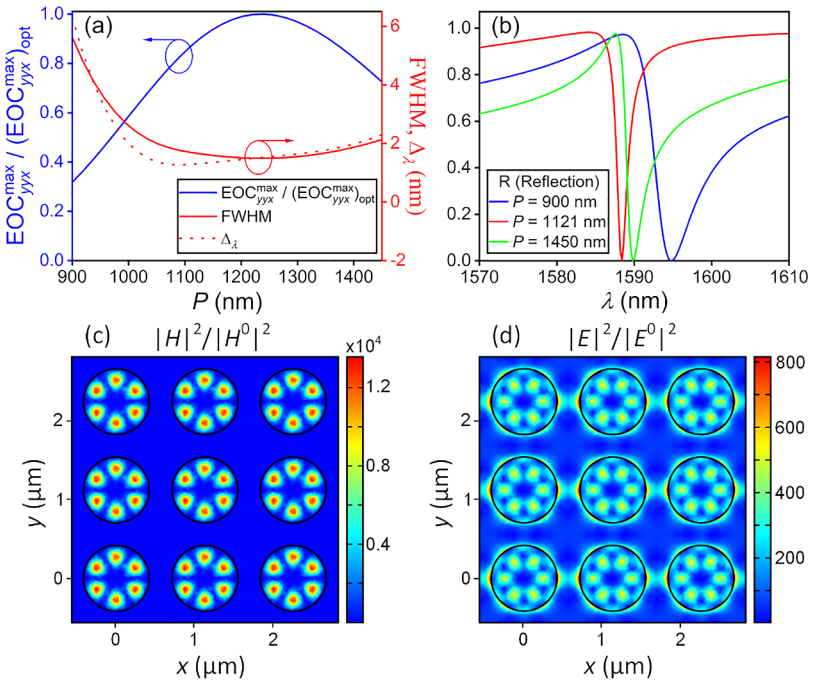


**Figure 4.** (a) Dependencies of the spectral maximum of component $EOC^{max}_{yyx}$ normalized to $(EOC^{max}_{yyx})_{opt}$, of the full width at half-maximum (FWHM) and shift $\Delta_\lambda = \lambda_R - \lambda_{oct}$ of the lattice octupole resonance on the lattice period, where the maximum possible value of octupole component $(EOC^{max}_{yyx})_{opt}$ corresponds to the period $P = 1221$ nm; $\lambda_{oct} = 1587$ nm for a single disk. (b) Reflection spectra in the vicinity of octupole resonance for different periods of lattice. Intensities of (c) magnetic and (d) electric fields (normalized to the corresponding values of the incident wave) in the metasurface plane (a several elementary cell presentation) at the octupole resonance.

$$\alpha_1 E_x^0 \simeq -\frac{\alpha_2}{\varepsilon_0} S^{FF}[O_{yyx} - O_{xxx}] \tag{6}$$

where $\alpha_1$ and $\alpha_2$ are the components of the dipole polarizability tensor $\hat{\alpha}_p$ for the frontal and lateral irradiations by the $x$-polarized plane wave, respectively. Here, we also introduced the far-field part of the EOC-ED sum

$$S^{FF} = \frac{k_0^2 k_d^2}{24\pi} \sum_{l\neq 0}^{\infty} x_l^2 y_l^2 \frac{e^{ik_d r_l}}{r_l^5} \tag{7}$$

where $(x_l, y_l)$ are the in-plane coordinates of the center of the disk with number $l$, $r_l = \sqrt{x_l^2 + y_l^2}$. Note that, since the coordinates $x_l$ and $y_l$ enter the sum in an even power, the sum $S^{FF}$ is not equal to zero confirming the presence of the dipole−octupole coupling in the metasurface.

For the estimation of eq 6, we introduce two coefficients

$$\Xi = |-\alpha_2 S^{FF}(O_{yyx} - O_{xxx})|/|\alpha_1 E_x^0| \tag{8a}$$

$$\Theta = \mathrm{Arg}(-\alpha_2 S^{FF}(O_{yyx} - O_{xxx})) - \mathrm{Arg}(\alpha_1 E_x^0) \tag{8b}$$

which characterize eq 8a, the ratio between the magnitudes of the ED moments excited in any disk of the metasurface by the external electric field and by the far fields generated by the EOC moments of other disks, and eq 8a, the phase difference $\Delta\phi$ between these ED moments ($\Theta = 0$ corresponds to $\Delta\phi = \pi$). The inset in Figure 3b demonstrates the spectral behavior of these coefficients. One can see that their values at the resonant wavelength $\lambda_R = 1588$ nm agree with the coupling model: $\Xi$ has a resonant peak with a value close to 0.25; $\Theta$ approaches zero at the resonant point.

The observed effect of dipole−octupole coupling is stable to the variations of the lattice period: the variations in the period on the order of hundreds of nanometers lead to changes in the wavelength of the octupole resonance and its quality factor by only a few nanometers (see Figure 4a,b). Importantly, this effect leads to significant magnetic and electric field enhancements in the metasurface plane (see Figure 4c,d). Note, if we neglect the small imaginary part of the $MoS_2$ permittivity in the simulation, then the quality factor of the EOC resonance only slightly increases. This is due to the leaky nature of the array's EOC mode and its radiation losses, which are determined by the irremovable contributions of weak multipoles of different orders. Thus, the additional optimization procedure could be applied for quality factor optimization (see Figure S6).

The considered metasurfaces can be used as a highly efficient ultrathin system for storing electromagnetic energy, as well as pumping 2D lasers. Their experimental implementation may involve the use of various substrates on which $MoS_2$ disks are deposited. From Figure 5, one can see that for low-refractive-index substrates, the studied octupole resonance is still observed; however, its manifestation decreases with increasing the substrate refractive index. Note that for the $SiO_2$ substrate, the reflection in the overall considered spectral range is significantly decreased due to the diffraction transmission into the substrate, and the resonant trapping effect disappears. The estimated value of the substrate refractive indexes $n_{sub}$, for which the trapping effect can be destroyed, is $n_{sub} \geq \lambda_p/P$, where $\lambda_p$ is the wavelength of the octupole resonance realized in the metasurface with the period $P$ and placed in a homogeneous environment with permittivity $\varepsilon_d = 1$. If the diffraction in a substrate is not realized, the EOC mode trapping effect can be obtained in a metasurface with specially optimized parameters (see Figure S7 where this effect is demonstrated for the metasurface composed of $MoS_2$ disks with a radius of 300 nm and a height of 400 nm and placed on


https://doi.org/10.1021/acsphotonics.2c01066
ACS Photonics XXXX, XXX, XXX−XXX

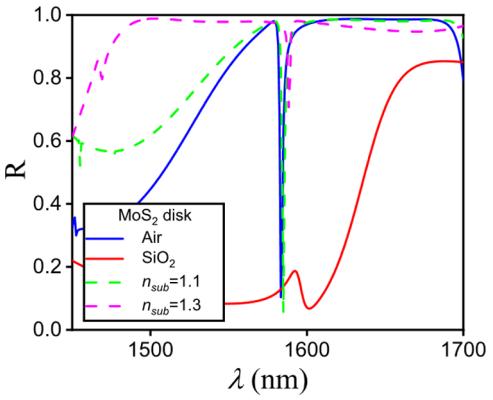


**Figure 5.** Spectral dependencies of the reflection coefficient ($R$) for metasurface composed of $MoS_2$ disks with optimized period $P$ = 1121 nm deposited on various substrates with the refractive index $n_{sub}$.

a $SiO_2$ substrate with a period of 800 nm). However, since the presence of the substrate breaks the out-of-plane symmetry, the amplitude and phase distributions of all multipole components can be changed compared with free space, resulting in another multipole coupling behavior.

## CONCLUSIONS

We considered the trapping mode effect in $MoS_2$ metasurfaces, the realization of which is determined by self-consisting coupling between broad dipole and narrow resonant octupole moments of the metasurface's building blocks. Since the coupling mechanism of the trapping is related to the excitation of certain eigenmodes of a cylindrical dielectric resonator, it can be implemented in various dielectric metasurfaces, whose building blocks support the resonant excitation of multipole moments with the same inverse symmetry property. As a result, the metasurface composed of silicon disks can also exhibit features associated with octupole resonance.

## ASSOCIATED CONTENT

### Supporting Information

The Supporting Information is available free of charge at https://pubs.acs.org/doi/10.1021/acsphotonics.2c01066.

$MoS_2$ relative permittivity; octupole resonance in Si disks; main equations of the multipole analysis; far-field approximation of the lattice EOC-ED sum; quality factor of octupole resonance in a metasurface; effect of the finite size of the metasurface array; and influence of the substrate on the octupole resonance in a metasurface (PDF)

## AUTHOR INFORMATION


### Corresponding Author

**Andrey B. Evlyukhin** − *Institute of Quantum Optics, Leibniz Universität Hannover, 30167 Hannover, Germany;* orcid.org/0000-0002-1801-6778; Email: a.b.evlyukhin@daad-alumni.de

### Authors

**Alexei V. Prokhorov** − *State Key Laboratory on Integrated Optoelectronics, College of Electronic Science and Engineering, International Center of Future Science, Jilin University, Changchun 130012, China*

**Pavel D. Terekhov** − *Department of Electrical Engineering, The Pennsylvania State University, University Park, Pennsylvania 16802, United States*

**Mikhail Yu. Gubin** − *State Key Laboratory on Integrated Optoelectronics, College of Electronic Science and Engineering, International Center of Future Science, Jilin University, Changchun 130012, China*

**Alexander V. Shesterikov** − *State Key Laboratory on Integrated Optoelectronics, College of Electronic Science and Engineering, International Center of Future Science, Jilin University, Changchun 130012, China*

**Xingjie Ni** − *Department of Electrical Engineering, The Pennsylvania State University, University Park, Pennsylvania 16802, United States;* orcid.org/0000-0001-7405-5678

**Vladimir R. Tuz** − *State Key Laboratory on Integrated Optoelectronics, College of Electronic Science and Engineering, International Center of Future Science, Jilin University, Changchun 130012, China;* orcid.org/0000-0001-6096-7465

Complete contact information is available at: https://pubs.acs.org/10.1021/acsphotonics.2c01066


### Notes

The authors declare no competing financial interest.

## ACKNOWLEDGMENTS

The authors are grateful for support from Jilin University, China. Support from the Deutsche Forschungsgemeinschaft (DFG, German Research Foundation) under Germany's Excellence Strategy within the Cluster of Excellence PhoenixD (EXC 2122, Project ID 390833453) is acknowledged.

## REFERENCES


(1) Silva, A.; Monticone, F.; Castaldi, G.; Galdi, V.; Alù, A.; Engheta, N. Performing mathematical operations with metamaterials. *Science* **2014**, *343*, 160−163.

(2) Ni, X.; Emani, N. K.; Kildishev, A. V.; Boltasseva, A.; Shalaev, V. M. Broadband light bending with plasmonic nanoantennas. *Science* **2012**, *335*, 427.

(3) Billings, L. Exotic optics: Metamaterial world. *Nature* **2013**, *500*, 138−140.

(4) Khanikaev, A. B.; Mousavi, S. H.; Tse, W.-K.; Kargarian, M.; MacDonald, A. H.; Shvets, G. Photonic topological insulators. *Nat. Mater.* **2013**, *12*, 233−239.

(5) Novotny, L.; Hecht, B.*Principles of Nano-Optics*; Cambridge University Press, 2012.

(6) Caputo, J.-G.; Gabitov, I.; Maimistov, A. I. Polarization rotation by an rf-SQUID metasurface. *Phys. Rev. B* **2015**, *91*, 115430.

(7) Liu, N.; Weiss, T.; Mesch, M.; Langguth, L.; Eigenthaler, U.; Hirscher, M.; Sönnichsen, C.; Giessen, H. Planar metamaterial analogue of electromagnetically induced transparency for plasmonic sensing. *Nano Lett.* **2010**, *10*, 1103−1107.

(8) Evlyukhin, A. B.; Bozhevolnyi, S. I.; Pors, A.; Nielsen, M. G.; Radko, I. P.; Willatzen, M.; Albrektsen, O. Detuned electrical dipoles for plasmonic sensing. *Nano Lett.* **2010**, *10*, 4571−4577.

(9) Evlyukhin, A. B.; Novikov, S. M.; Zywietz, U.; Eriksen, R. L.; Reinhardt, C.; Bozhevolnyi, S. I.; Chichkov, B. N. Demonstration of magnetic dipole resonances of dielectric nanospheres in the visible Region. *Nano Lett.* **2012**, *12*, 3749−3755.

(10) Rybin, M. V.; Koshelev, K. L.; Sadrieva, Z. F.; Samusev, K. B.; Bogdanov, A. A.; Limonov, M. F.; Kivshar, Y. S. High-Q supercavity modes in subwavelength dielectric resonators. *Phys. Rev. Lett.* **2017**, *119*, 243901.

(11) Koshelev, K.; Kivshar, Y. Dielectric resonant metaphotonics. *ACS Photonics* **2021**, *8*, 102−112.

(12) Bonod, N.; Kivshar, Y. All-dielectric Mie-resonant metaphotonics. *C. R. Phys.* **2020**, *21*, 425−442.
(13) Li, S.; Zhou, C.; Liu, T.; Xiao, S. Symmetry-protected bound states in the continuum supported by all-dielectric metasurfaces. *Phys. Rev. A* **2019**, *100*, 063803.
(14) Evlyukhin, A. B.; Tuz, V. R.; Volkov, V. S.; Chichkov, B. N. Bianisotropy for light trapping in all-dielectric metasurfaces. *Phys. Rev. B* **2020**, *101*, 205415.
(15) Prokhorov, A. V.; Shesterikov, A. V.; Gubin, M. Y.; Volkov, V. S.; Evlyukhin, A. B. Quasitrapped modes in metasurfaces of anisotropic $MoS_2$ nanoparticles for absorption and polarization control in the telecom wavelength range. *Phys. Rev. B* **2022**, *106*, 035412.
(16) Hsu, C. W.; Zhen, B.; Stone, A. D.; Joannopoulos, J. D.; Soljačić, M. Bound states in the continuum. *Nat. Rev. Mater.* **2016**, *1*, 16048.
(17) Joseph, S.; Pandey, S.; Sarkar, S.; Joseph, J. Bound states in the continuum in resonant nanostructures: an overview of engineered materials for tailored applications. *Nanophotonics* **2021**, *10*, 4175−4207.
(18) Vabishchevich, P. P.; Liu, S.; Sinclair, M. B.; Keeler, G. A.; Peake, G. M.; Brener, I. Enhanced second-harmonic generation using broken symmetry III-V semiconductor Fano metasurfaces. *ACS Photonics* **2018**, *5*, 1685−1690.
(19) Li, G.-C.; Lei, D.; Qiu, M.; Jin, W.; Lan, S.; Zayats, A. V. Light-induced symmetry breaking for enhancing second-harmonic generation from an ultrathin plasmonic nanocavity. *Nat. Commun.* **2021**, *12*, No. 4326.
(20) Zograf, G.; Koshelev, K.; Zalogina, A.; Korolev, V.; Hollinger, R.; Choi, D.-Y.; Zuerch, M.; Spielmann, C.; Luther-Davies, B.; Kartashov, D.; et al. High-harmonic generation from resonant dielectric metasurfaces empowered by bound states in the continuum. *ACS Photonics* **2022**, *9*, 567−574.
(21) Tuz, V. R.; Prosvirnin, S. L.; Kochetova, L. A. Optical bistability involving planar metamaterials with broken structural symmetry. *Phys. Rev. B* **2010**, *82*, 233402.
(22) Tuz, V. R.; Butylkin, V. S.; Prosvirnin, S. L. Enhancement of absorption bistability by trapping-light planar metamaterial. *J. Opt.* **2012**, *14*, 045102.
(23) Evlyukhin, A. B.; Poleva, M. A.; Prokhorov, A. V.; Baryshnikova, K. V.; Miroshnichenko, A. E.; Chichkov, B. N. Polarization switching between electric and magnetic quasi-trapped modes in bianisotropic all-dielectric metasurfaces. *Laser Photonics Rev.* **2021**, *15*, 2100206.
(24) Kauranen, M.; Zayats, A. V. Nonlinear plasmonics. *Nat. Photonics* **2012**, *6*, 737−748.
(25) Vaskin, A.; Kolkowski, R.; Koenderink, A. F.; Staude, I. Light-emitting metasurfaces. *Nanophotonics* **2019**, *8*, 1151−1198.
(26) Ha, S. T.; Fu, Y. H.; Emani, N. K.; Pan, Z.; Bakker, R. M.; Paniagua-Domínguez, R.; Kuznetsov, A. I. Directional lasing in resonant semiconductor nanoantenna arrays. *Nat. Nanotechnol.* **2018**, *13*, 1042−1047.
(27) Kodigala, A.; Lepetit, T.; Gu, Q.; Bahari, B.; Fainman, Y.; Kanté, B. Lasing action from photonic bound states in continuum. *Nature* **2017**, *541*, 196−199.
(28) Azzam, S. I.; Chaudhuri, K.; Lagutchev, A.; Kim, Y. L.; Shalaev, V. M.; Boltasseva, A.; Kildishev, A. V. In *Room-Temperature Lasing Action from All-Dielectric Metasurfaces Near Bound States in the Continuum*, Conference on Lasers and Electro-Optics, Washington, DC, 2020.
(29) Wu, M.; Ha, S. T.; Shendre, S.; Durmusoglu, E. G.; Koh, W.-K.; Abujetas, D. R.; Sánchez-Gil, J. A.; Paniagua-Domínguez, R.; Demir, H. V.; Kuznetsov, A. I. Room-temperature lasing in colloidal nanoplatelets via Mie-resonant bound states in the continuum. *Nano Lett.* **2020**, *20*, 6005−6011.
(30) Fedotov, V. A.; Rose, M.; Prosvirnin, S. L.; Papasimakis, N.; Zheludev, N. I. Sharp trapped-mode resonances in planar metamaterials with a broken structural symmetry. *Phys. Rev. Lett.* **2007**, *99*, 147401.
(31) Zhang, J.; MacDonald, K. F.; Zheludev, N. I. Near-infrared trapped mode magnetic resonance in an all-dielectric metamaterial. *Opt. Express* **2013**, *21*, 26721−26728.
(32) Koshelev, K.; Lepeshov, S.; Liu, M.; Bogdanov, A.; Kivshar, Y. Asymmetric metasurfaces with high-*Q* resonances governed by bound states in the continuum. *Phys. Rev. Lett.* **2018**, *121*, 193903.
(33) Tuz, V. R.; Khardikov, V. V.; Kupriianov, A. S.; Domina, K. L.; Xu, S.; Wang, H.; Sun, H.-B. High-quality trapped modes in all-dielectric metamaterials. *Opt. Express* **2018**, *26*, 2905−2916.
(34) Tsilipakos, O.; Maiolo, L.; Maita, F.; Beccherelli, R.; Kafesaki, M.; Kriezis, E. E.; Yioultsis, T. V.; Zografopoulos, D. C. Experimental demonstration of ultrathin broken-symmetry metasurfaces with controllably sharp resonant response. *Appl. Phys. Lett.* **2021**, *119*, 231601.
(35) Han, S.; Pitchappa, P.; Wang, W.; Srivastava, Y. K.; Rybin, M. V.; Singh, R. Extended bound states in the continuum with symmetry-broken terahertz dielectric metasurfaces. *Adv. Opt. Mater.* **2021**, *9*, 2002001.
(36) van Hoof, N. J.; Abujetas, D. R.; Ter Huurne, S. E.; Verdelli, F.; Timmermans, G. C.; Sánchez-Gil, J. A.; Rivas, J. G. Unveiling the symmetry protection of bound states in the continuum with terahertz near-field imaging. *ACS Photonics* **2021**, *8*, 3010−3016.
(37) Babicheva, V. E.; Evlyukhin, A. B. Multipole lattice effects in high refractive index metasurfaces. *J. Appl. Phys.* **2021**, *129*, 040902.
(38) Ermolaev, G. A.; Grudinin, D. V.; Stebunov, Y. V.; Voronin, K. V.; Kravets, V. G.; Duan, J.; Mazitov, A. B.; Tselikov, G. I.; Bylinkin, A.; Yakubovsky, D. I.; Novikov, S. M.; Baranov, D. G.; Nikitin, A. Y.; Kruglov, I. A.; Shegai, T.; Alonso-González, P.; Grigorenko, A. N.; Arsenin, A. V.; Novoselov, K. S.; Volkov, V. S. Giant optical anisotropy in transition metal dichalcogenides for next-generation photonics. *Nat. Commun.* **2021**, *12*, No. 854.
(39) Terekhov, P. D.; Babicheva, V. E.; Baryshnikova, K. V.; Shalin, A. S.; Karabchevsky, A.; Evlyukhin, A. B. Multipole analysis of dielectric metasurfaces composed of nonspherical nanoparticles and lattice invisibility effect. *Phys. Rev. B* **2019**, *99*, 045424.
(40) Miroshnichenko, A. E.; Evlyukhin, A. B.; Yu, Y. F.; Bakker, R. M.; Chipouline, A.; Kuznetsov, A. I.; Luk'yanchuk, B.; Chichkov, B. N.; Kivshar, Y. S. Nonradiating anapole modes in dielectric nanoparticles. *Nat. Commun.* **2015**, *6*, No. 8069.


https://doi.org/10.1021/acsphotonics.2c01066
ACS Photonics XXXX, XXX, XXX−XXX